Figures and figure supplements

PtdInsP$_2$ and PtdSer cooperate to trap synaptotagmin-1 to the plasma membrane in the presence of calcium

Ángel Pérez-Lara *et al*

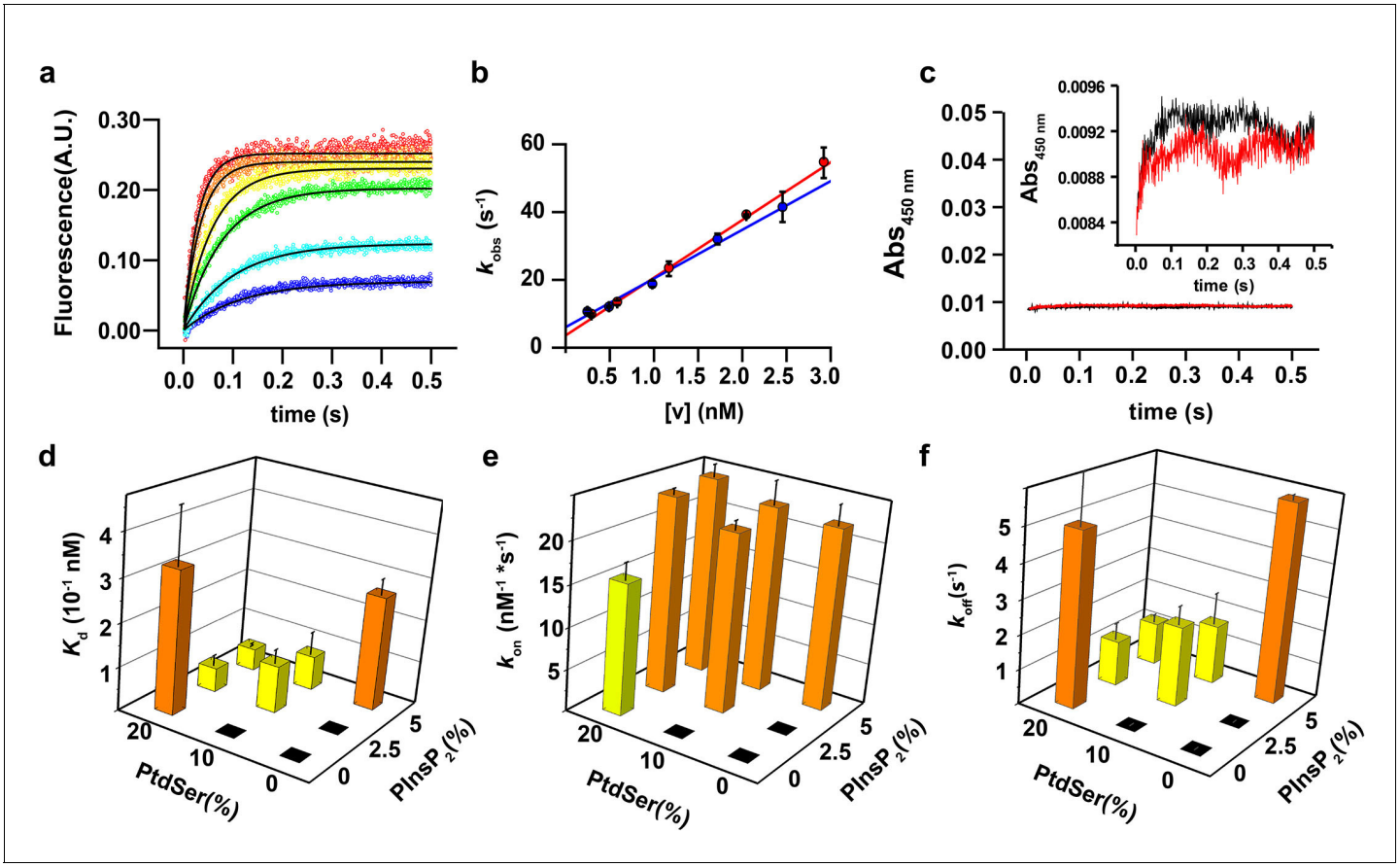

Figure 1. PtdIns(4,5)P_2 and PtdSer act cooperatively in the membrane binding of the C2AB fragment. (**a**) Representative time courses of dansyl emission for rapid mixing of 0.25 μM syt-1 C2AB fragment (final concentration) with increasing concentrations of large unilamellar vesicles (final liposome concentrations ranging between 0.3 nM and 3 nM) containing PtdChol:PtdSer (80:20, molar ratio), measured at 25°C. The apparent rate constant k_{obs} was determined by fitting the traces to a monoexponential function (solid black lines). (**b**) The dependence of k_{obs} on the vesicle concentration: data from two different sets of liposomes used for the stopped-flow experiment shown in (a). The non-zero y-intercept of the linear regression curve yields k_{off} and the slope yields k_{on}. (**c**) Representative absorbance time course (n = 2) for rapid mixing of C2AB fragment (0.25 μM, final concentration) and vesicles (~2.5 nM). Absorbance was monitored at 450 nm for vesicles containing PtdChol/PtdSer/PtdIns(4,5)P_2 (75:20:5, molar ratio). No aggregation of vesicles was observed in our conditions, even when lipid mixtures with the highest affinity to C2AB fragment were used. (Inset) A scale-up of the traces showing that there is no vesicle aggregation in our conditions in concordance to the results of ***Vennekate et al. (2012)***. (**d**) K_d values, calculated as the ratio of k_{off}/k_{on}, (**e**) k_{on} and (**f**) k_{off} of C2AB fragment binding to liposomes containing different concentrations of PtdSer and PtdIns(4,5)P_2. All values were calculated from stopped-flow experiments carried out by rapid mixing of C2AB fragment with vesicles containing different amounts of PtdSer and/or PtdIns(4,5)P_2, and 100 μM free Ca^{2+} at 25°C (n = 5–10). Higher affinities (lower K_d) were observed in the presence of both PtdSer and PtdIns(4,5)P_2, solely resulting from a decrease in k_{off}. Columns with the same color indicate values that were not significantly different from each other. Black boxes indicate either lack of binding or low binding that was too noisy for a reliable quantitative analysis.

DOI: 10.7554/eLife.15886.003

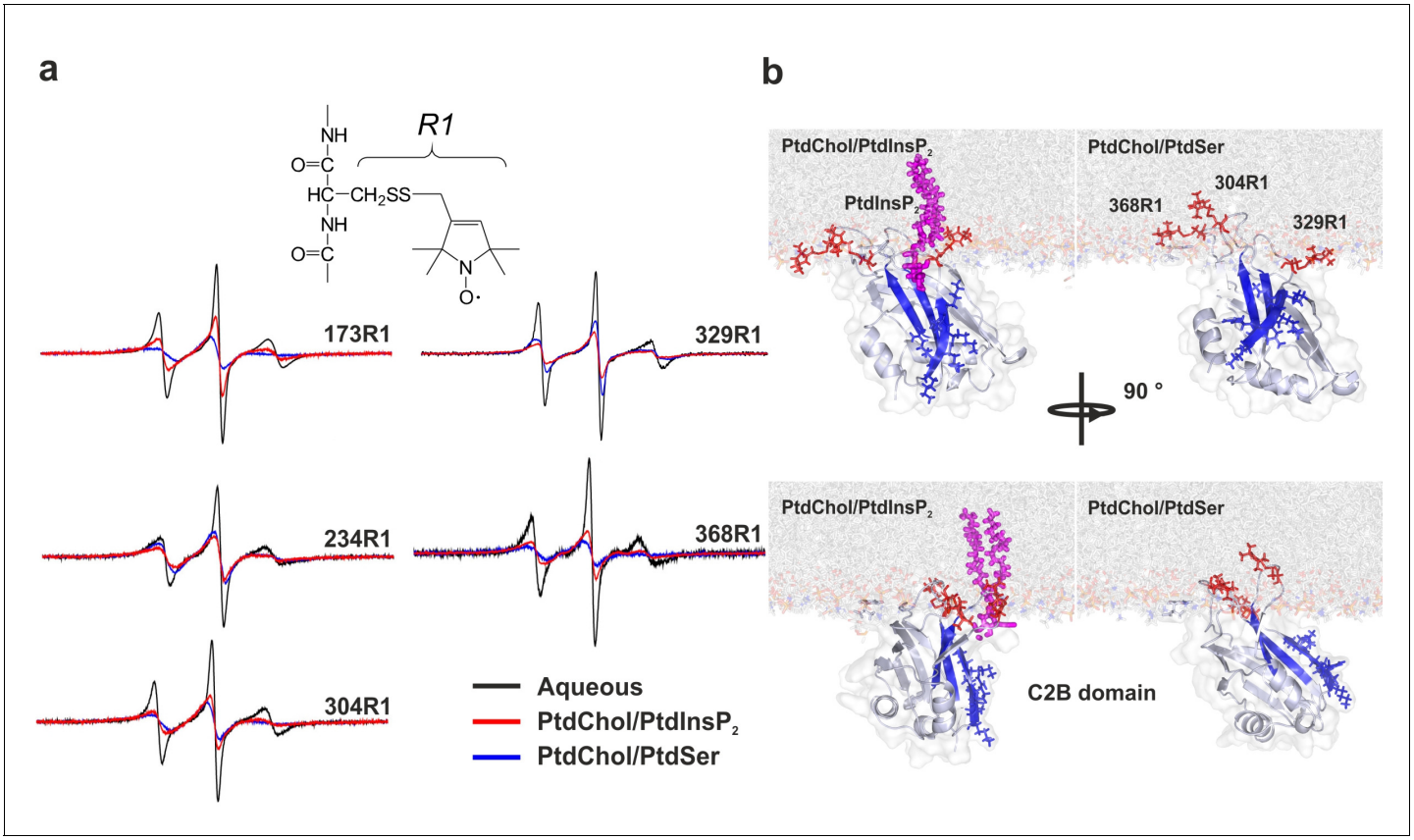

Figure 2. Orientation of the C2 domains bound to membranes containing either PtdSer or PtdIns(4,5)P_2. (**a**) EPR spectra from sites 173, 234, 304, 329 and 368 in solution or bound to bilayers containing PtdChol/PtdSer (80:20, molar ratio) or PtdChol/PtdInsP_2 (95:5, molar ratio). The broader spectra reflect diminished amplitudes and rates of R1 label motion when the C2AB fragment is bound to vesicles containing PtdChol/PtdIns(4,5)P_2 (95:5, molar ratio) or PtdChol/PtdSer (80:20, molar ratio) (n = 2–3). R1 is the spin-labeled side chain produced by derivatizing cysteine with the MTSL spin label. (**b**) Docking orientation of the C2B domain (PDB ID: 1K5W [***Fernandez et al., 2001***]) at the membrane interface, polybasic patch in blue. In this figure, the result from Xplor-NIH (Materials and methods) was aligned with a membrane simulation generated by CHARMM-GUI (***Jo et al., 2008***) for a bilayer with PtdChol:PtdInsP_2 or PtdChol:PtdSer at a molar ratio of 97:3 or 80:20, respectively. PtdIns(4,5)P_2 (pink sticks) was manually docked to the C2B domain. Blue sticks correspond to residues 321–326 and red sticks correspond to R1-labeled residues used in EPR experiments.

DOI: 10.7554/eLife.15886.004

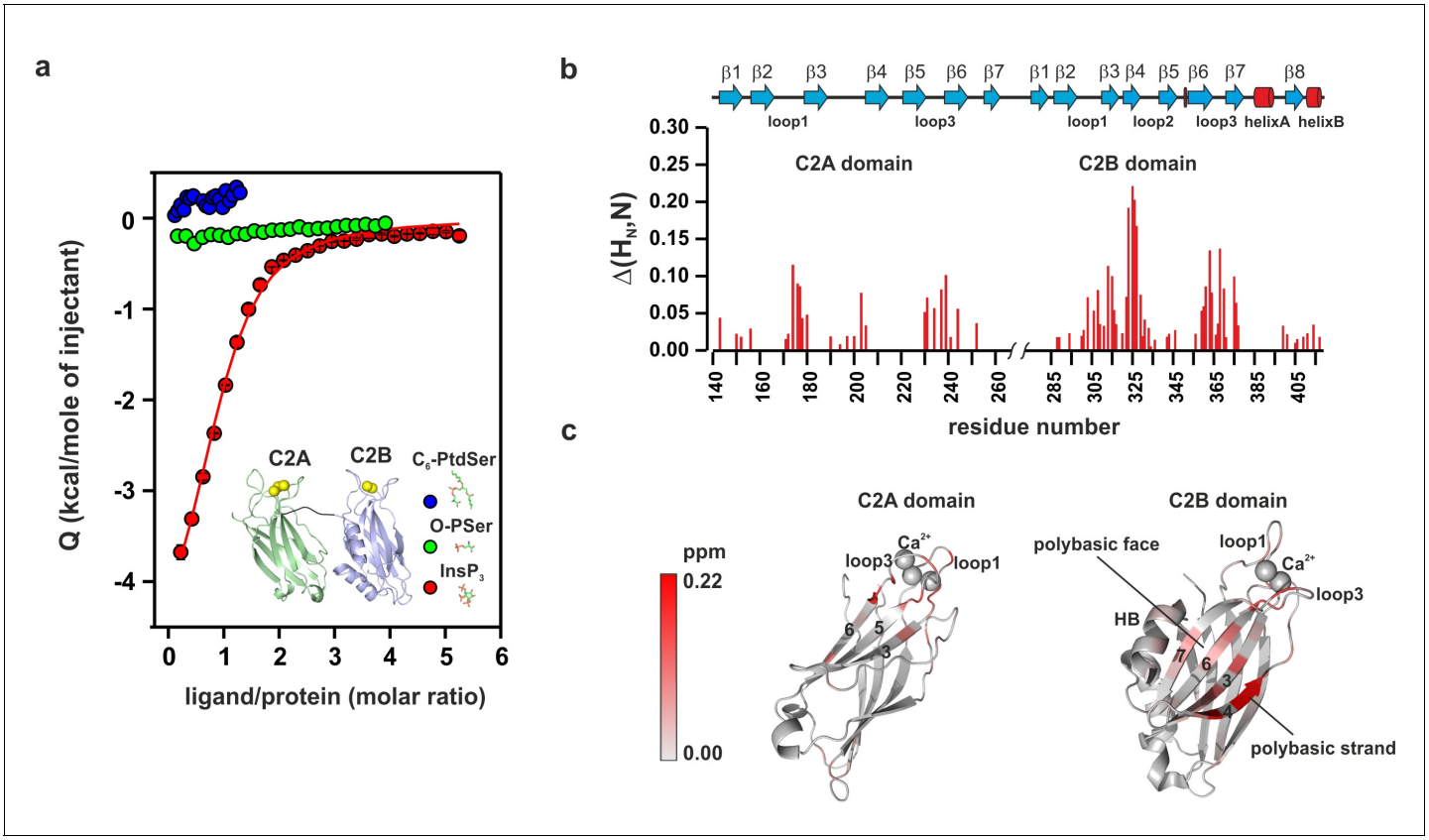

Figure 3. PtdIns(4,5)P_2 binds preferentially to the polybasic patch of the C2B domain. (**a**) Binding of the C2AB fragment to phospholipid head groups measured by isothermal titration calorimetry (ITC). Titration of ~50 µM C2AB fragment (50 mM HEPES, pH 7.4, 150 mM NaCl and 1 mM $CaCl_2$) with $InsP_3$ (inositol-1,4,5-triphosphate) (n = 3), O-phosphoserine (O-PSer) (n = 2) and 1,2-hexanoyl-sn-glycero-3-phospho-L-serine (C_6-PtdSer) (n = 2), in the presence of saturating Ca^{2+} at 25°C. Only small heats were observed upon addition of C_6-PtdSer and O-PSer, while $InsP_3$ binds specifically (K_d = 14 ± 2 µM) with a stoichiometry of 1:1. (**b**) Averaged-weighted chemical shifts (ΔH_N, N) in ^{15}N-^{1}H correlated HSQC NMR spectra of syt-1 in the presence of $InsP_3$ and Ca^{2+}. Chemical shift changes are widely distributed in the polybasic region of C2B domain. Small chemical shift are also seen in the calcium-binding loops of the C2B and C2A domains. Measurements were made under normal ionic strength (150 mM NaCl, 50 mM MES, pH = 6.3, and 3 mM Ca^{2+}) at a frequency of 600 MHz for protons. (**c**) Chemical shifts are color coded and mapped onto the structures of C2B and C2A domains according to the color bar (n = 2–3).

DOI: 10.7554/eLife.15886.006

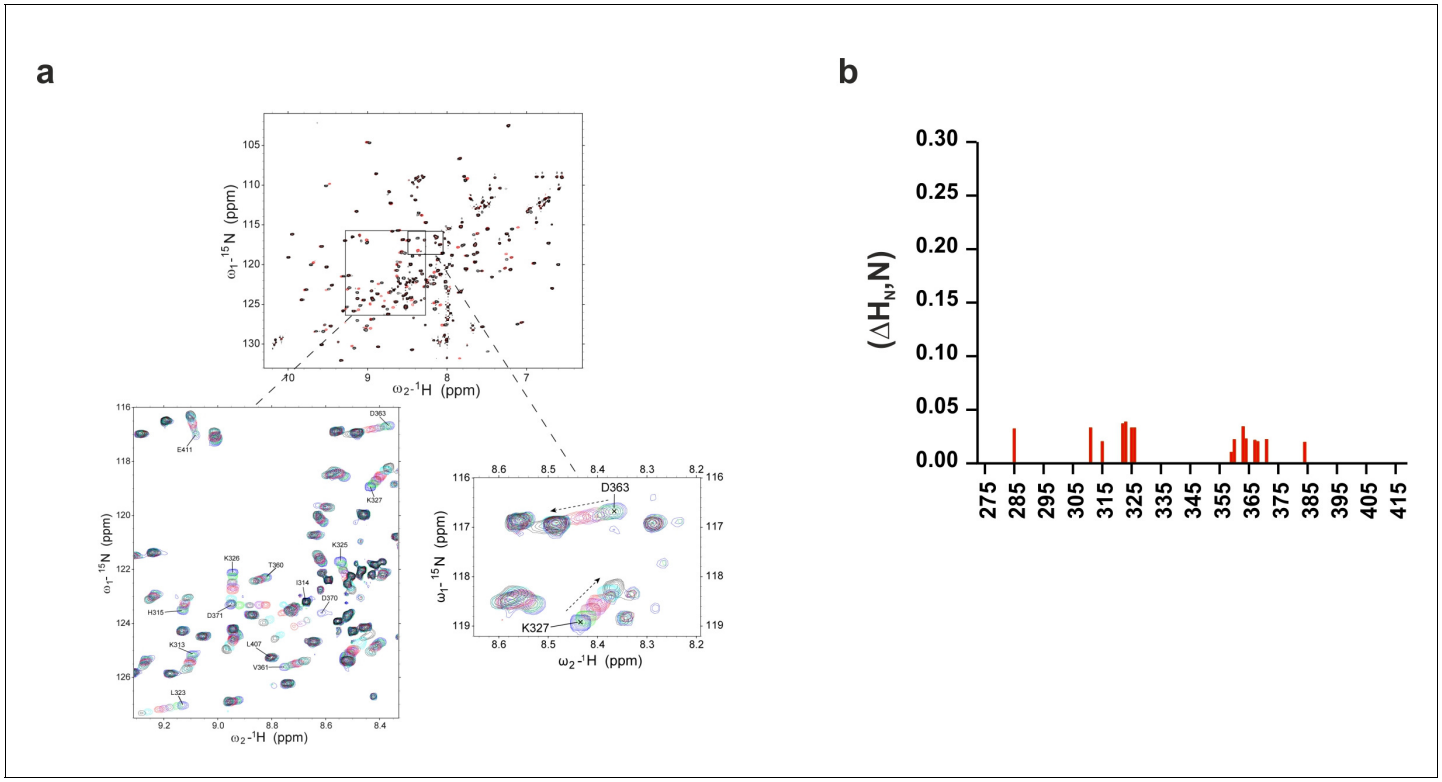

Figure 3—figure supplement 1. Chemical shift of ^{1}H-^{15}N HSQC of C2B domain in the presence of $InsP_3$ or O-PSer. (**a**) Chemical shifts of ^{1}H-^{15}N HSQC of C2AB fragment in the absence (black) and in the presence of 2 mM $InsP_3$ (red). The expanded section of the HSQC spectrum shows chemical shift changes upon titration with different concentrations of $InsP_3$ (0 mM, blue; 0.1 mM, green; 0.2 mM, maroon; 0.3 mM, purple; 0.5 mM, red; 1 mM, cyan and 2 mM, black). (**b**) Average weighted chemical shifts (ΔH_N,N) in the presence of 7 mM O-phosphoserine. Measurements are made under normal ionic strength conditions (150 mM NaCl, 50 mM MES, pH = 6.3, and 3 mM Ca^{2+}) at a frequency of 600 MHz for protons.

DOI: 10.7554/eLife.15886.007

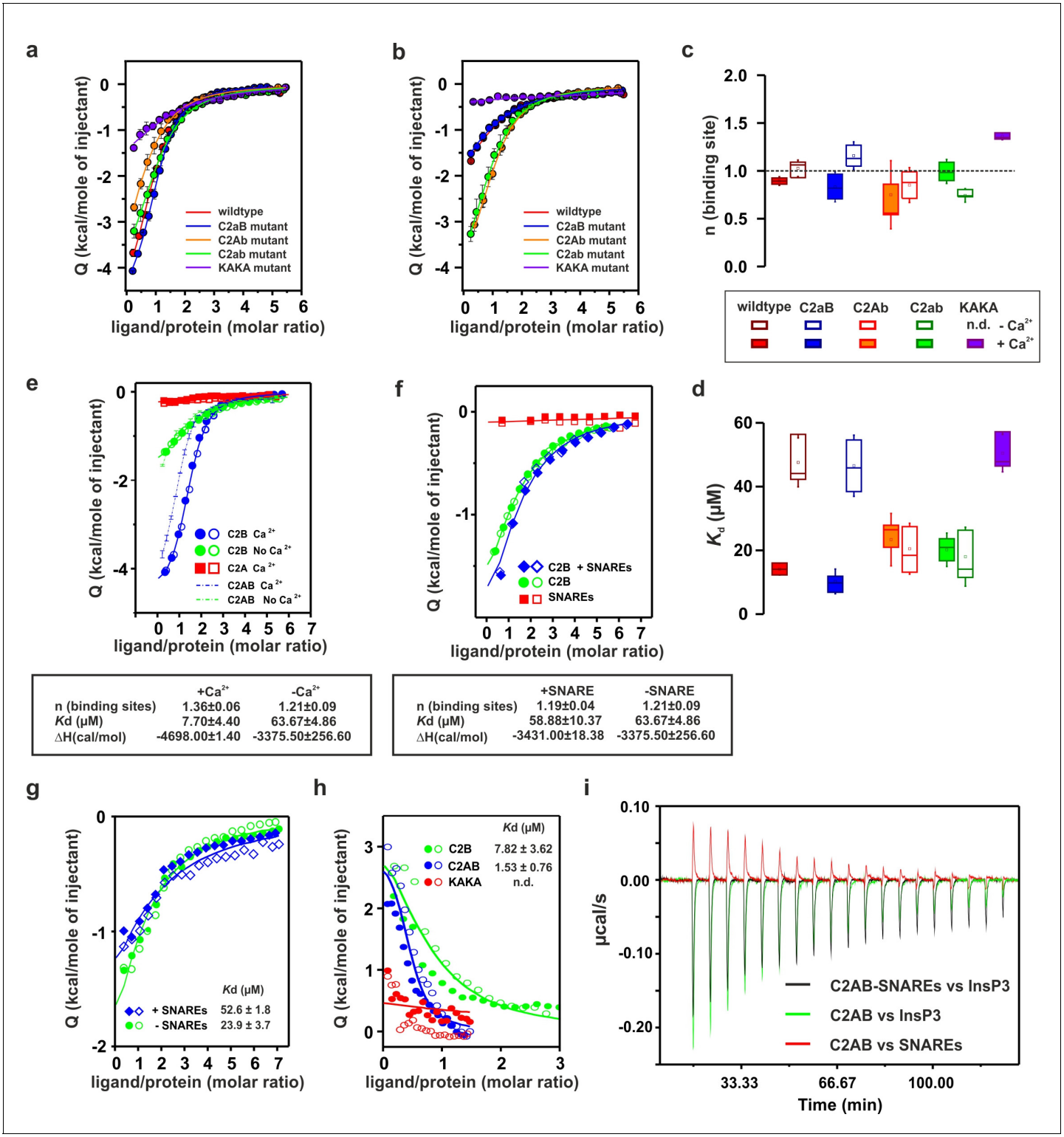

Figure 4. Ca^{2+} increases the affinity of PtdIns(4,5)P_2 to the polybasic patch by means of shielding the negative charges of the Ca^{2+}-binding site in the C2B domain. (**a**,**b**) Representative ITC titrations (n = 3–6) of ~50 μM of the wild-type C2AB fragment, mutant proteins in which either one or both Ca^{2+} binding sites are mutated, and the KAKA mutant in which some of the charges in the polybasic patch are removed. Titrations were carried out with $InsP_3$ as shown in ***Figure 3a*** in (**a**) the presence or (**b**) the absence of Ca^{2+}. Lines represent the fitting of the different titrations. (**c**) Number of binding sites determined from the fits of the ITC experiments of the different C2 domains shown in (**a**) and (**b**). All C2 domains show one binding site for $InsP_3$ in the presence or absence of Ca^{2+}. In absence of Ca^{2+}, binding of $InsP_3$ to the KAKA mutant was completely abolished. (**d**) Dissociation constants (K_d)

Figure 4 continued on next page

Figure 4 continued

calculated from the experiments shown in (a) and (b). In the presence of Ca^{2+}, only the KAKA mutant shows a significant decrease in the binding to $InsP_3$. In the absence of Ca^{2+}, mutations in the C2B Ca^{2+}-binding site rescue the binding to $InsP_3$, where as the KAKA mutant shows weak unspecific binding. (**e**) Titration of ~50 μM C2A domain (in the presence of Ca^{2+}) and C2B domain (in the presence or absence of Ca^{2+}) with $InsP_3$ (n = 2) compared to that of the C2AB fragment in same conditions (see legend). The C2B domain is responsible for $InsP_3$ binding to syt-1. (**f**) Titration of ~50 μM C2B domain–SNARE-complex (1:1, molar ratio) with $InsP_3$ in the absence of Ca^{2+} (n = 2). The C2B domain binds preferentially to $InsP_3$ in physiological conditions. (**g**) Titration of ~15 μM C2AB domain/SNARE-complex (1:1, molar ratio) with $InsP_3$ in the absence of Ca^{2+} (n = 2). We set the number sites to one for the fitting due to the uncertainty resulting from the low concentrations used. (**h**) Titration of SNARE-complex ~15 μM with different syt-1 fragments in the absence of Ca^{2+} (n = 2). The K_d values from (**g**) and (**h**) should be interpreted with caution because the low concentration used for the titrations resulted in a high uncertainty on the fitting. (**i**) Representative raw data for titration from (**g**) and (**h**). Interestingly, titration of the C2AB–SNARE complex presented an endothermic profile, whereas titration of $InsP_3$ presented an exothermic profile.
DOI: 10.7554/eLife.15886.008

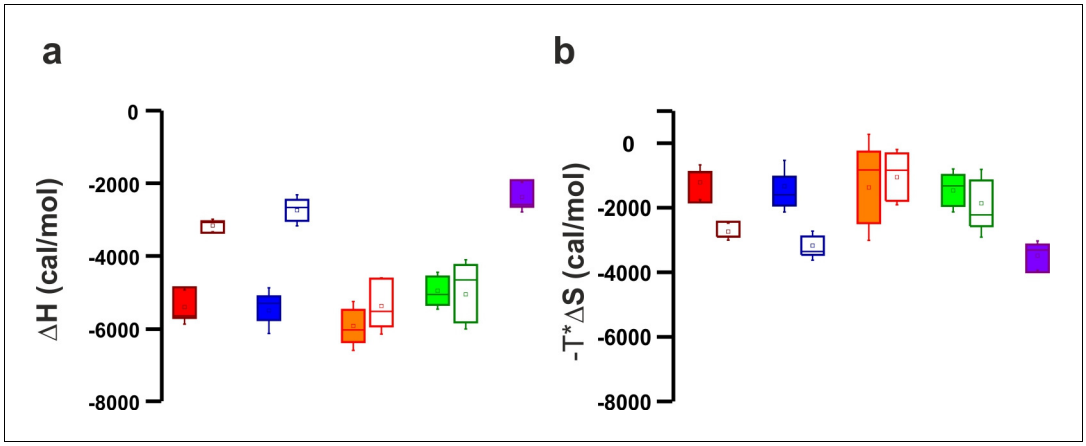

Figure 4—figure supplement 1. Thermodinamic binding parameters of the different C2AB fragments. (**a**) Binding enthalpy (△H) and (**b**) entropy (-T*△S) for ITC titration in ***Figure 4a,b***.
DOI: 10.7554/eLife.15886.009

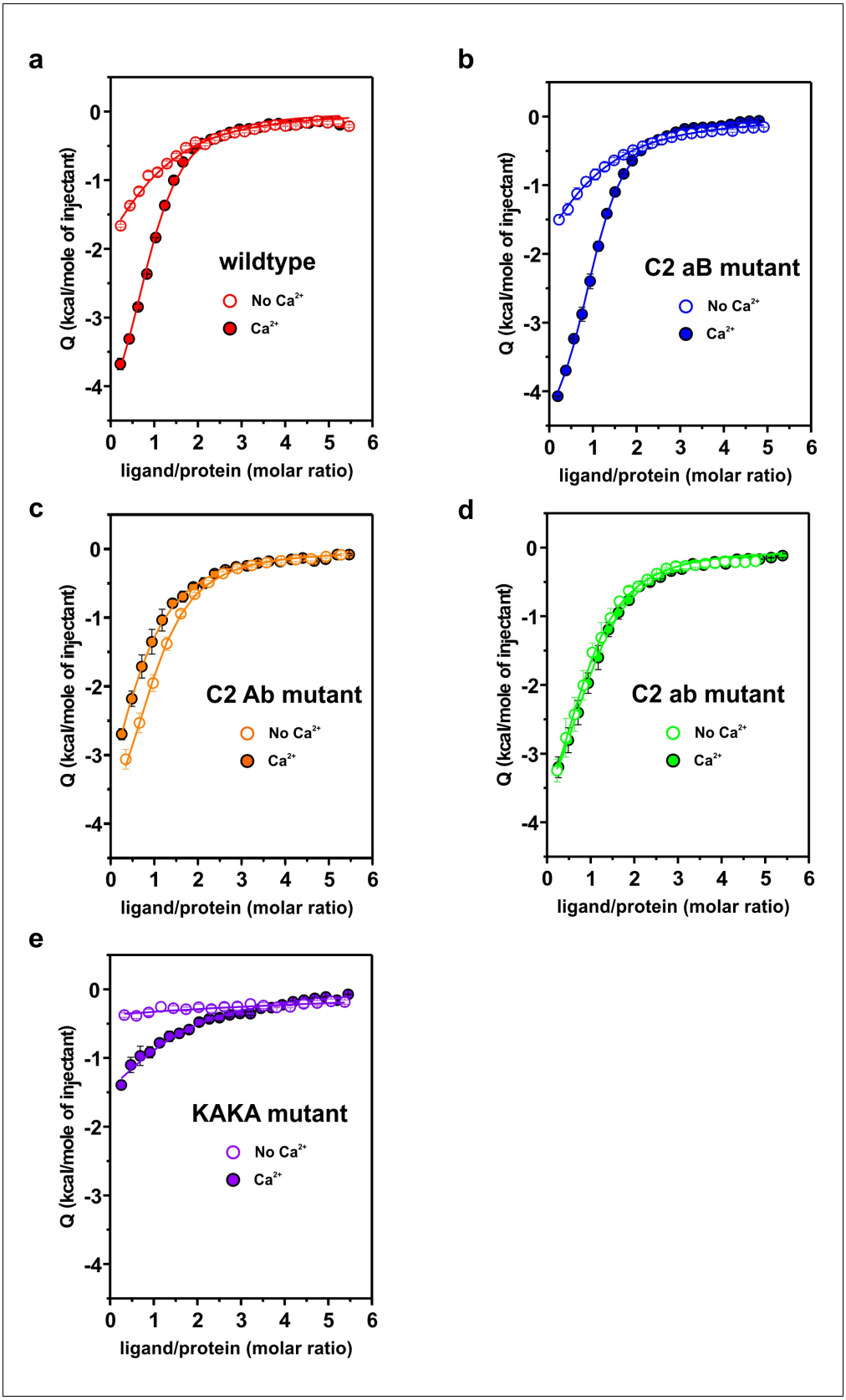

Figure 4—figure supplement 2. Representative titrations (n ≥ 3) of ~50 μM of the C2AB fragment used in ***Figure 4a,b*** in the presence or absence of Ca^{2+}.

Figure 4—figure supplement 2 continued on next page

Figure 4—figure supplement 2 continued

DOI: 10.7554/eLife.15886.010

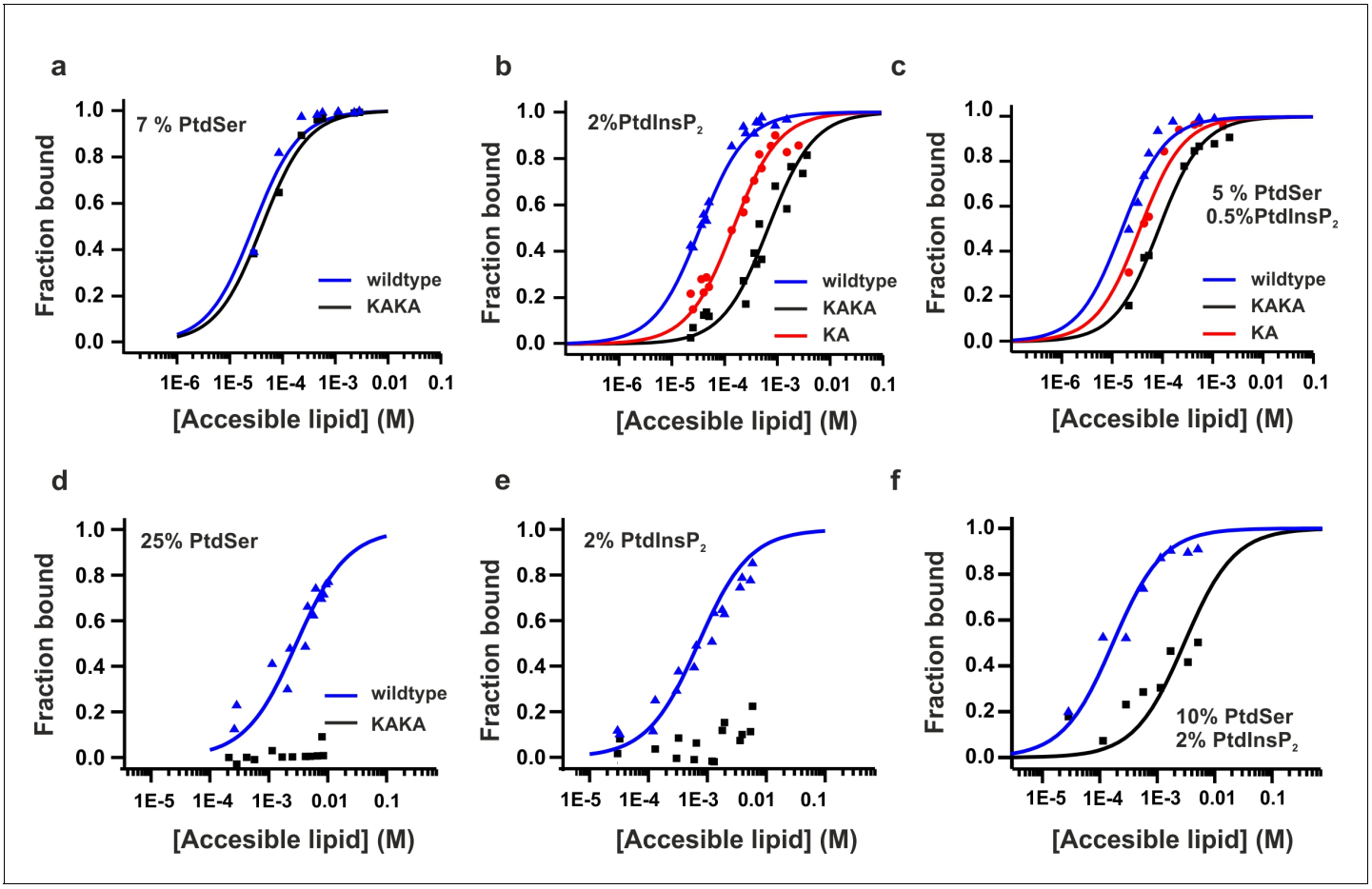

Figure 5. Equilibrium binding of the C2AB fragment and polybasic mutants to PtdChol, PtdSer and PtdIns(4,5)P_2 bilayers. (**a**,**b**,**c**) Ca^{2+}-dependent and (d,e,f) Ca^{2+}-independent partitioning of C2AB fragment into (**a**,**d**) PtdChol/PtdSer, (**b**,**e**) PtdChol/ PtdIns(4,5)P_2 and (**c**,**f**) PtdChol/PtdSer/ PtdIns(4,5)P_2 bilayers. (d,e) No binding of the KAKA mutant was observed in the presence of PtdSer or PtdIns(4,5)P_2 alone in absence of calcium . At equivalent charge densities, removal of lysine residues within the polybasic face reduced the membrane affinity in vesicles containing PtdSer and PtdIns (4,5)P_2 (**c**) more than it did in vesicles containing either (**a**) PtdSer or(**b**) PtdIns (4,5)P_2 in the presence of calcium. The lines represent fits to the data using Eq [1] (Materials and methods). Reciprocal molar partition coefficients obtained from data are listed in ***Tables 2*** and ***3*** (n = 2–3).

DOI: 10.7554/eLife.15886.011

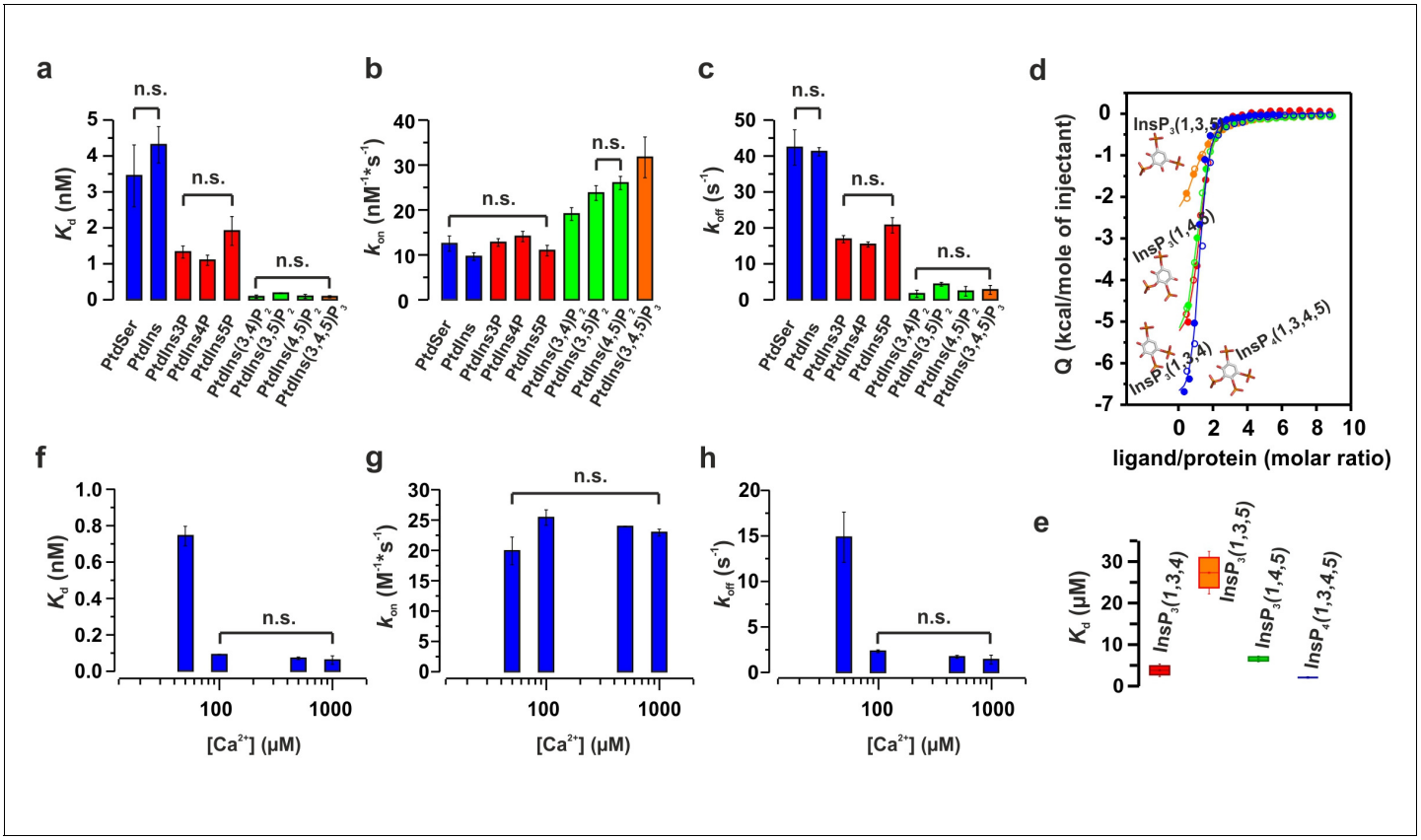

Figure 6. Ca^{2+} and phosphoinositides increase the membrane affinity of syt-1 by decreasing the dissociation rate of the syt-1–membrane complex. (**a**) K_d, (**b**) k_{on} and (**c**) k_{off} calculated from stopped-flow experiments carried out by rapid mixing, as in ***Figure 1***, of C2AB fragment with vesicles containing PtdChol/PtdSer/PtdEth/Chol/$PtdInsP_X$ (55:11:22:11:1 molar ratio), where X = 0–3 phosphate groups, in 20 mM HEPES (pH 7.4), 150 mM KCl, 1 mM EGTA and 1.1 mM $CaCl_2$ (100 μM free Ca^{2+}) at 37°C (n = 5–10). An increased number of phospho groups of phosphoinositides increases the affinity by decreasing the dissociation rate (k_{off}). A minor increase in k_{on} was detected in the case of $PtdInsP_{2–3}$. (**d**) Thermodynamic characterization of the binding of C2B domain to head groups of physiological phosphoinositides by ITC. Titration of ~50 μM C2B domain (50 mM HEPES (pH 7.4), 150 mM NaCl and 1 mM $CaCl_2$) with main stereoisomers of $InsP_{3–4}$ at 25°C (n = 2).(**e**) Dissociation constants (K_d) calculated for experiments from d. (**f**) K_d, (**g**) k_{on} and (**h**) k_{off} calculated from stopped-flow experiments carried out at different Ca^{2+}concentrations with vesicles containing PtdChol/PtdSer/PtdEth/Chol/PtdIns(4,5)P_2 (55:11:22:11:1 molar ratio) at 37°C (n = 5–10). Ca^{2+} decreases the rate of dissociation drastically (**h**) and thereby increases the affinity (**f**). No significant difference was observed for the rate of association (k_{on}) (**g**).

DOI: 10.7554/eLife.15886.014

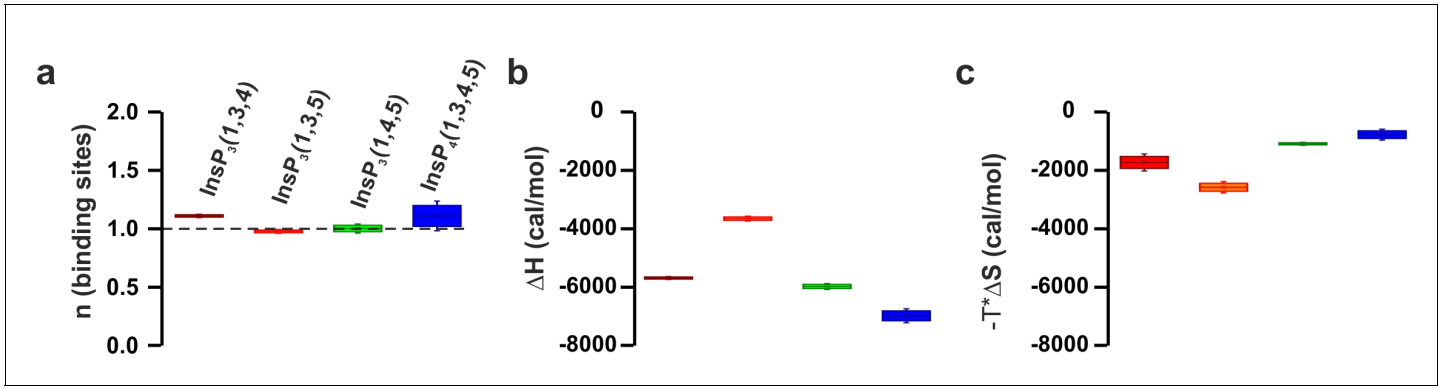

Figure 6—figure supplement 1. ITC parameters of the C2B domain binding to different isomers of $InsP_3$. (**a**) Number of binding sites, (**b**) binding enthalpy (△H) and (**c**) entropy (-T*△S) for ITC titration in ***Figure 6d***. Titration of ~50 μM C2B domain (in the presence of Ca^{2+}) with different isomers of $InsP_3$.

DOI: 10.7554/eLife.15886.015

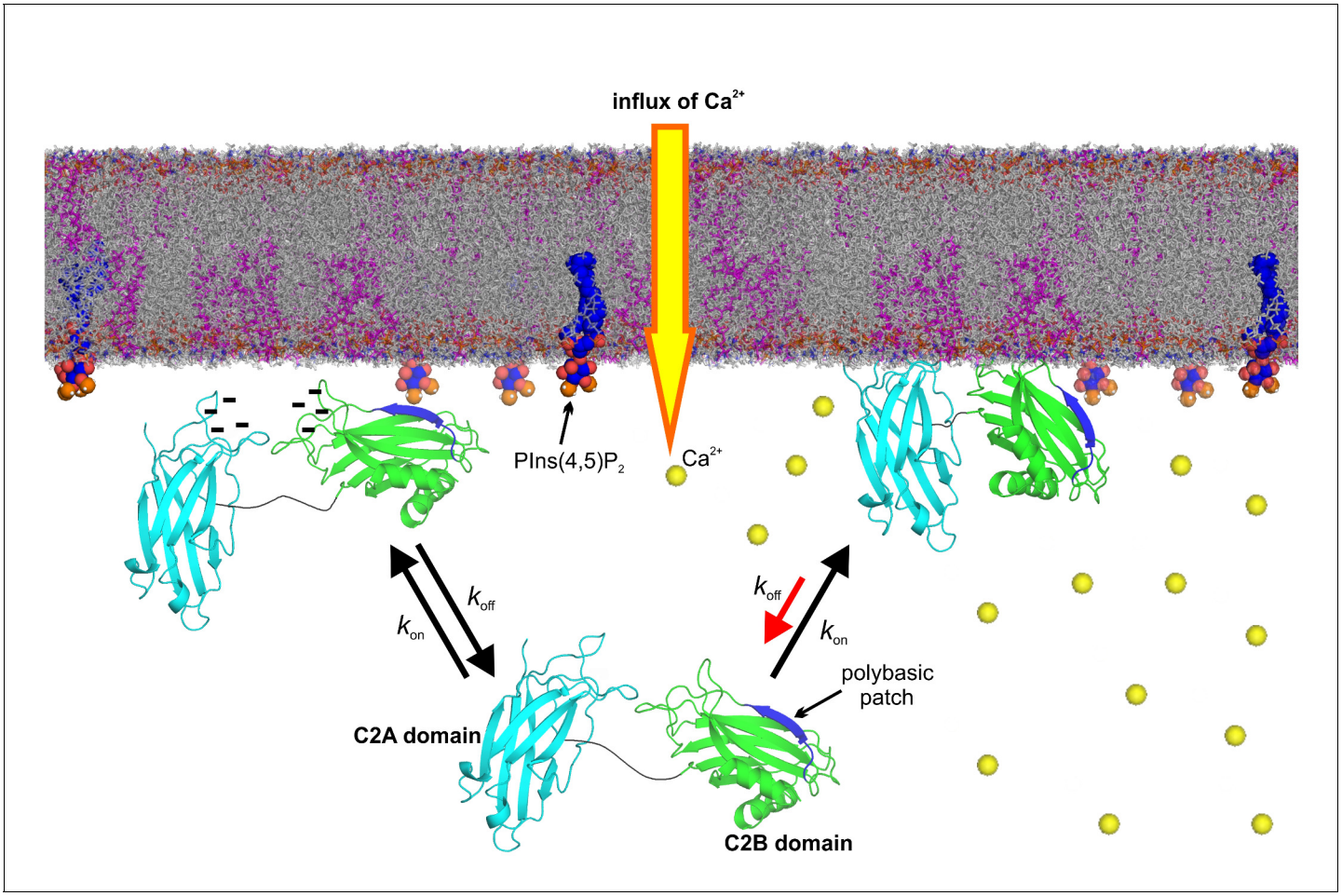

Figure 7. Model of the membrane-binding mechanism of syt-1. In the absence of Ca^{2+}, syt-1 is attached to the presynaptic membrane interface. Syt-1 binds to PtdIns(4,5)P_2 through its C2B polybasic patch (***Bai et al., 2004***; ***Kuo et al., 2009***) in transient encounters, but the negative charges of the Ca^{2+}-binding pockets prevent penetration of the C2 domains into the presynaptic membrane because of the electrostatic repulsion between them, leading to a high rate of dissociation. Upon Ca^{2+} influx, Ca^{2+} binding neutralizes the negative charge of the Ca^{2+}-binding sites. As a consequence, phosphatidylserine completes the sphere of coordination of Ca^{2+} and allows the insertion of the hydrophobic residues at the tips of the C2 domains. Simultaneously, the polybasic patch enhances its affinity to phosphoinositides, leading to deeper penetration of the C2B Ca^{2+}-binding site into the bilayer. Together, these events decrease the rate of dissociation of syt-1 from the membrane and enhance its penetration into the core of the presynaptic membrane, which eventually leads to SNARE-mediated membrane fusion. Nuclear magnetic resonance structures of the C2A domain (PDB 1BYN [***Shao et al., 1998***]) and C2B domain (1K5W [***Fernandez et al., 2001***]) of syt-1 and a molecular dynamic membrane simulation were rendered using PyMOL Molecular Graphics System (Schrödinger,LLC, http://www.pymol.org). The membrane used in this illustration was generated using the Membrane Builder input generator module in CHARMM-GUI (***Jo et al., 2008***) for a bilayer with PtdChol:PhdSer:PtdEth:Chol:PtdInsP_2 at a molar ratio of 55:11:22:11:1.

DOI: 10.7554/eLife.15886.016